Solid State Ionics 32/33 (1989) 904–910
North-Holland, Amsterdam

THE INTERACTION OF V_2O_5 AND Nb_2O_5 WITH OXIDE SURFACES

Israel E. WACHS, Jih-Mirn JEHNG and Franklin D. HARDCASTLE
Zettlemoyer Center for Surface Studies, Department of Chemical Engineering and Chemistry, Lehigh University, Bethlehem, PA 18015, USA

Received 23 June 1988; accepted for publication 24 June 1988

The interaction of vanadium oxide and niobium oxide with Al_2O_3 and TiO_2 supports is examined with Raman spectroscopy. The Raman spectra of the supported metal oxides reveal that the strong interaction of the metal oxides with Al_2O_3 and TiO_2 supports results in the formation of two-dimensional surface metal oxide overlayers. The surface vanadium oxide overlayers are unstable to high calcination temperatures and readily undergo solid state transformations. The surface niobium oxide overlayers are much more stable to high-temperature calcination treatments and retard solid state transformations of the mixed oxide systems.

1. Introduction

Supported metal oxides are formed when one metal oxide phase is dispersed onto a second metal oxide substrate. The dispersed supported metal oxide phase can simultaneously possess several different molecular states. The multiple molecular states that can simultaneously coexist in the supported metal oxide phase have generated confusion in the understanding of supported metal oxide materials. This confusion has resulted primarily because of the lack of applicable characterization techniques capable of discriminating between these different molecular states. Conventional characterization techniques provide general information concerning the physical characteristics of the supported metal oxide phase, but are not adequate to discriminate between the different molecular states that are simultaneously present [1]. In the past few years, however, characterization studies of supported metal oxides have shown that the different molecular states in the supported metal oxide phase can be discriminated with the use of laser Raman spectroscopy [2,3]. This technique can readily discriminate between the different molecular states of the supported metal oxides because each state possesses a unique vibrational spectrum that is related to its structure. Therefore, Raman spectroscopy provides direct information about the structure of each state as well as a method of discriminating between the various states.

In the present investigation we report on the Raman spectroscopy of supported vanadium oxide and supported niobium oxide on Al_2O_3 and TiO_2 supports. The influence of the oxide supports and calcination temperature upon the structural nature of the supported vanadium oxide and niobium oxide phases will be discussed. The vanadium oxide and niobium oxide systems were simultaneously investigated in order to highlight the similarities and differences between these two supported group VB metal oxides.

2. Experimental

The supported metal oxide catalysts were prepared by the incipient-wetness impregnation method. The oxide supports consist of γ-Al_2O_3 (Harshaw, 180 m^2/g) and TiO_2 (Degussa P-25, anatase/rutile ≈ 2, 55 m^2/g). The V_2O_5/TiO_2 samples were made with $VO(OC_2H_5)_3$ (Alfa) in ethanol, dried at room temperature for 16 h, dried at 110–120°C for 16 h, and calcined at 450°C for 2 h. The V_2O_5/Al_2O_3 samples were made with $VO(OC_3H_7)_3$ (Alfa) in methanol, dried at room temperature for 16 h, dried at 110–120°C for 16 h, and calcined at 450°C for 16 h. The Nb_2O_5/TiO_2 and Nb_2O_5/Al_2O_3 samples were synthesized from $Nb(HC_2O_4)_5$ (Niobium Products Co.,

Pittsburgh, PA) in oxalic acid solution. The supported niobium oxide samples were subsequently dried at 110–120°C for 16 h, and calcined at 500°C (Nb_2O_5/Al_2O_3, 16 h; Nb_2O_5/TiO_2, 2 h). Several of the above samples were further calcined at higher temperatures in order to examine the influence of calcination temperature upon the supported vanadium oxide and niobium oxide systems. The sample surface areas were measured with a Quantisorb BET apparatus using N_2 gas. The Raman apparatus has been described elsewhere [2].

3. Results and discussion

3.1. Supported vanadium oxide

The interaction of vanadium oxide with the Al_2O_3 support is shown in the Raman spectra presented in fig. 1. The nature of the supported vanadium oxide phase is determined by comparison of the Raman spectra of the supported vanadium oxide sample with spectra of vanadium oxide reference compounds [4–9]. The 3–20% V_2O_5/Al_2O_3 samples do not contain the Raman features of either crystalline V_2O_5 (major bands at 1000, 703, 525, and 150 cm^{-1}) or $AlVO_4$ (major bands at 1017, 988, 899, 510, 391, 319, 279, and 133 cm^{-1}), but possess weak and broad Raman bands characteristic of surface vanadate species. The two-dimensional surface vanadate overlayer possesses coverage-dependent Raman bands in the 900–1000 cm^{-1} region which are characteristic of symmetric V=O stretching modes and bands at ≈ 500 and 220 cm^{-1} which are characteristic of V–O–V linkages. Above 20% V_2O_5/Al_2O_3, the Raman spectra exhibit the strong and sharp features diagnostic of crystalline V_2O_5 which overshadow the weaker Raman features of the surface vanadate overlayer. Thus, a monolayer of the surface vanadate species on alumina corresponds to ≈20% V_2O_5/Al_2O_3 for this system. A closer examination of the Raman spectra below monolayer coverage reveals that the 10 and 20% V_2O_5/Al_2O_3 spectra possess more pronounced features and additional bands than in the 3 and 5% V_2O_5/Al_2O_3 spectra. These differences suggest that the nature of the surface vanadate species on Al_2O_3 changes with surface coverage. Additional insight into the molecular structure of the surface vanadate overlayer in V_2O_5/Al_2O_3 is obtained from ^{51}V solid state NMR experiments [10]. The solid state NMR measurements reveal that two different surface vanadate structures exist on the alumina surface and that their relative concentrations depend on surface coverage. Below 10% V_2O_5/Al_2O_3, a tetrahedral surface vanadate species possessing two terminal oxygen atoms is present. At 10–20% V_2O_5/Al_2O_3 a second surface vanadate species is also present possessing a square-pyramidal structure (VO_5; similar to that found in bulk V_2O_5).

The Raman spectra for the supported vanadium oxide on TiO_2 samples are presented in fig. 2. In general, the very strong TiO_2 Raman features below 700

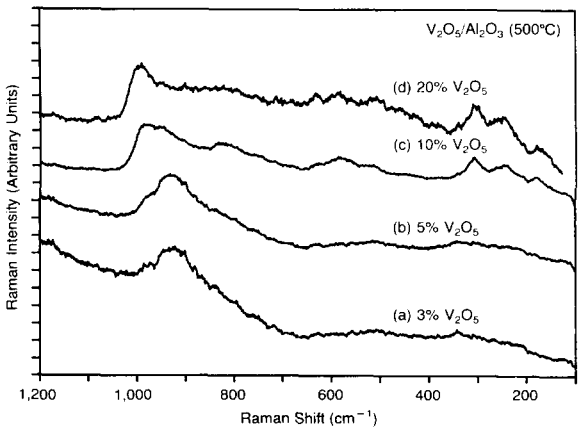

Fig. 1. Raman spectra for V_2O_5/Al_2O_3 (500°C) as a function of vanadia coverage: (a) 3% V_2O_5, (b) 5% V_2O_5, (c) 10% V_2O_5, and (d) 20% V_2O_5.

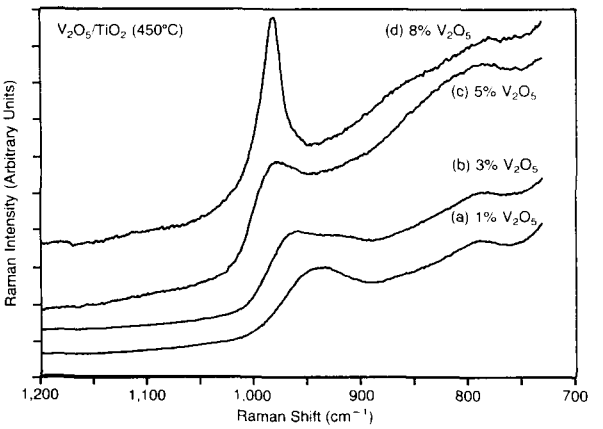

Fig. 2. Raman spectra for V_2O_5/TiO_2 (450°C) as a function of vanadia coverage: (a) 1% V_2O_5, (b) 3% V_2O_5, (c) 5% V_2O_5, and (d) 8% V_2O_5.

cm^{-1} prevent the acquisition of Raman spectra in this region for supported metal oxides on TiO_2. Furthermore, the TiO_2 support possesses a weak band at ≈ 796 cm^{-1} which arises from the first overtone of its very strong band at 398 cm^{-1}. The 1–5% V_2O_5/TiO_2 samples do not exhibit the Raman features of crystalline V_2O_5, but possess the weak and broad Raman bands characteristic of a two-dimensional surface vanadate phase. The surface vanadate species exhibit coverage-dependent Raman bands in the 900–1000 cm^{-1} region which are characteristic of the symmetric V=O stretching modes. The Raman spectrum of the 8% V_2O_5/TiO_2 sample is dominated by the strong and sharp band of crystalline V_2O_5 at 1000 cm^{-1} and overshadows the weaker Raman features of the surface vanadate species. Thus, a monolayer of the surface vanadate on titania corresponds to $\approx 7\%$ V_2O_5/TiO_2 for this system. Additional insight into the molecular structure of the surface vanadate overlayer in V_2O_5/TiO_2 is obtained from ^{51}V solid state NMR experiments and reveals that the square-pyramidal VO_5 surface vanadate species is much more prominent on the TiO_2 support than on the Al_2O_3 support at comparable surface coverages of vanadium oxide [10].

The influence of elevated calcination temperatures upon the V_2O_5/Al_2O_3 and V_2O_5/TiO_2 systems was also investigated. Both of these supported vanadium oxide systems exhibit very dramatic decreases in surface area upon calcination between 700 and 950°C, and the corresponding surface areas are shown in table 1. Note that the presence of the supported vanadium oxide phase dramatically accelerates the loss in surface area of both the Al_2O_3 and TiO_2 supports. The significant loss in surface area of the oxide supports serves to increase the surface density of the two-dimensional vanadate overlayer and transforms the surface vanadium oxide species to crystalline V_2O_5. This is shown in the Raman spectra of 5% V_2O_5/Al_2O_3 calcined at 500°C and 950°C in fig. 3 where the surface vanadate overlayer is transformed to crystalline V_2O_5 by the heat treatment. The supported crystalline V_2O_5 is stable on the Al_2O_3 support and does not undergo any solid state reactions with the alumina support at elevated temperatures (crystalline $AlVO_4$ is not stable at elevated temperatures). Thus, the loss in surface area of the V_2O_5/Al_2O_3 system at elevated temperatures results in a phase separation of the V_2O_5 and Al_2O_3 components. The influence of calcination temperature upon the V_2O_5/TiO_2 system is somewhat more complicated as shown in the Raman spectra of 5% V_2O_5/TiO_2, calcined at 450°C and 850°C in fig. 4. The supported crystalline V_2O_5 is unstable on the TiO_2 support upon calcining at 850°C as demonstrated by the absence of the Raman band due to crystalline V_2O_5 at 1000 cm^{-1}; the 5% V_2O_5/TiO_2 sample undergoes a solid state reaction with the titania support to form crystalline $V_xTi_{1-x}O_2$ (rutile) with simultaneous reduction of the vanadium from the +5 to the +4 oxidation state. The $V_xTi_{1-x}O_2$ (rutile) solid solution has been well documented in the literature [6,9,11–14]. Thus, the V_2O_5/TiO_2 system undergoes a solid state reaction at elevated temperatures to form a single mixed oxide phase. These

Table 1
Influence of calcination temperature on surface area of supported vanadium oxide on TiO_2 and Al_2O_3.

Sample	Calcination temperature [a]			
	450°C	700°C	850°C	950°C
TiO_2	56 m^2/g	31 m^2/g	12 m^2/g	–
5% V_2O_5/TiO_2	46 m^2/g	17 m^2/g	5 m^2/g	–
Al_2O_3	180 m^2/g	–	–	94 m^2/g
5% V_2O_5/Al_2O_3	178 m^2/g	–	–	3 m^2/g

[a] TiO_2 samples calcined for 2 h; Al_2O_3 samples calcined for 16 h.

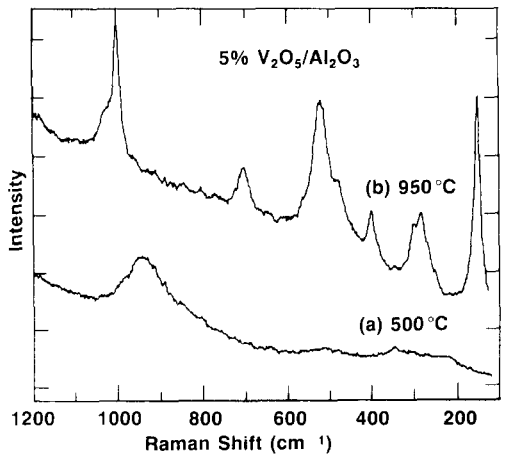

Fig. 3. Raman spectra for 5% V_2O_5/Al_2O_3 as a function of calcination temperature: (a) 500°C and (b) 950°C.

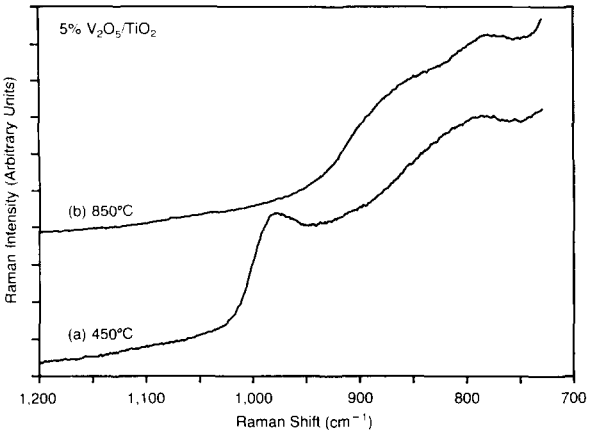

Fig. 4. Raman spectra for 5% V_2O_5/TiO_2 as a function of calcination temperature: (a) 450°C and (b) 850°C.

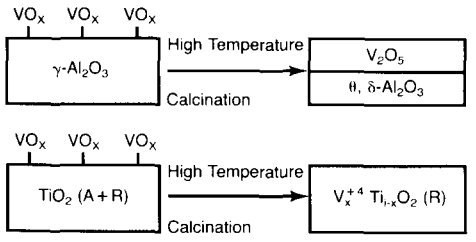

Fig. 5. Model of the interaction of vanadium oxide with oxide supports.

structural transformations are schematically depicted in fig. 5.

3.2. Supported niobium oxide

The interaction of niobium oxide with the Al_2O_3 support is shown in the Raman spectra presented in fig. 6. The nature of the supported niobium oxide phase is determined from a comparison of the Raman spectra of the supported niobium oxide samples with those of niobium oxide reference compounds [15,16]. The 1–19% Nb_2O_5/Al_2O_3 samples do not contain the Raman features of either the crystalline Nb_2O_5 phases (major band at ≈ 690 cm^{-1} due to NbO_6 octahedra) or $AlNbO_4$ (major bands at 931, 423, and 253 cm^{-1}), but possess weak and broad Raman bands characteristic of a two-dimensional surface niobate species. The surface niobate overlayer exhibits coverage-dependent Raman bands in

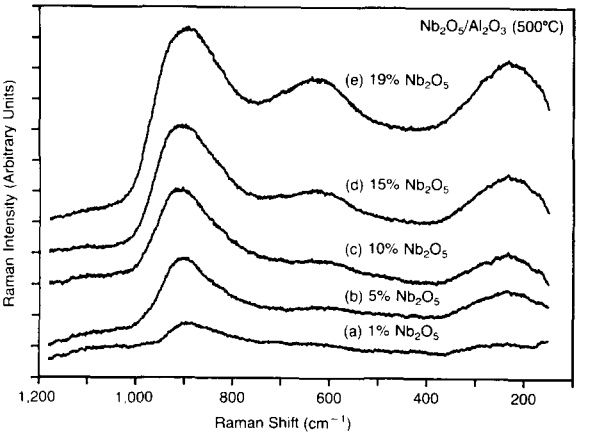

Fig. 6. Raman spectra for Nb_2O_5/Al_2O_3 (500°C) as a function of niobia coverage: (a) 1% Nb_2O_5, (b) 5% Nb_2O_5, (c) 10% Nb_2O_5, (d) 15% Nb_2O_5, and (e) 19% Nb_2O_5.

the 890–920 cm^{-1} region which are characteristic of the symmetric Nb=O stretching modes and bands at ≈ 230 cm^{-1} which are characteristic of Nb–O–Nb linkages. The molecular structure of the surface niobate species giving rise to the 890–920 cm^{-1} band is not completely understood at present (either a distorted octahedral or distorted tetrahedral structure). At niobium oxide contents of 10–19% Nb_2O_5/Al_2O_3 a pronounced Raman band at ≈ 630 cm^{-1} is also present. This additional Raman band at ≈ 630 cm^{-1} is due to an octahedrally coordinated surface niobate species that is present in the surface niobate overlayer at high surface coverages. Thus, similar to the V_2O_5/Al_2O_3 system, it appears that two different surface niobate species are present on the alumina support and that their relative concentrations are dependent on the surface coverage of the surface niobate species.

The Raman spectra for the supported niobium oxide on TiO_2 samples are presented in fig. 7. The 1–8% Nb_2O_5/TiO_2 samples give rise to extremely weak (especially against the TiO_2 background) and broad Raman bands in the 890–950 cm^{-1} region. These Raman bands are characteristic of a two-dimensional surface niobate species and are consistent with symmetric Nb=O stretching modes. The very strong TiO_2 Raman features below 700 cm^{-1} prevent the acquisition of additional Raman bands of the surface niobate phase and consequently the possible identification of Nb_2O_5 crystalline phases. X-ray dif-

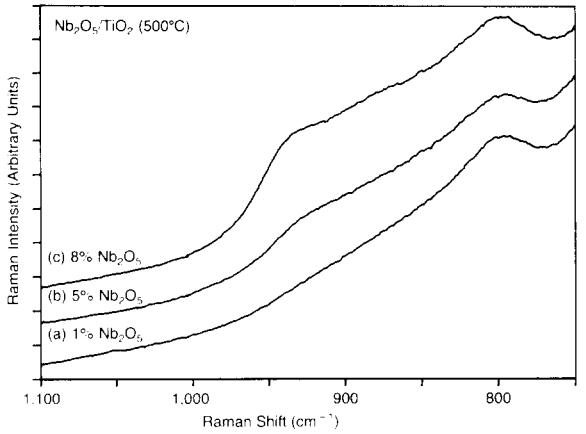

Fig. 7. Raman spectra for Nb_2O_5/TiO_2 (500°C) as a function of niobia coverage: (a) 1% Nb_2O_5, (b) 5% Nb_2O_5, and (c) 8% Nb_2O_5.

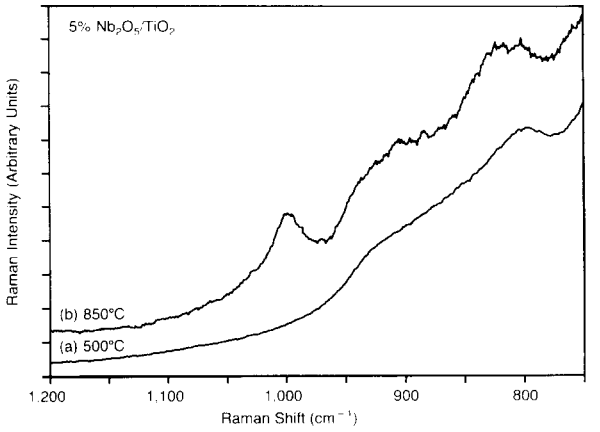

Fig. 8. Raman spectra for 5% Nb_2O_5/Al_2O_3 as a function of calcination temperature: (a) 500°C and (b) 950°C.

fraction analysis of the Nb_2O_5/TiO_2 samples did not reveal the presence of Nb_2O_5 crystallites.

The behavior of the Nb_2O_5/Al_2O_3 and Nb_2O_5/TiO_2 systems at elevated calcination temperatures is strikingly different from that of the corresponding supported V_2O_5 systems. The presence of the surface niobium oxide overlayer retards the loss in surface areas of the Al_2O_3 and TiO_2 supports at elevated calcination temperatures as shown in table 2. The influence of these high-temperature treatments upon the surface niobium oxide phases is shown in the Raman spectra of figs. 8 and 9. The Raman spectra of the 5% Nb_2O_5/Al_2O_3 sample calcined at 500 and 950°C (see fig. 8) reveal that the surface niobium oxide overlayer is present in both samples, and there is no evidence for the formation of crystalline Nb_2O_5 or $AlNbO_4$ phases. The additional Raman bands in the 950°C calcined sample are due to the transformation of the γ-Al_2O_3 support, which does not give rise to Raman signals, to δ-Al_2O_3, which gives rise to major bands at 253, 750, and 843 cm^{-1} [2]. In contrast to the V_2O_5/Al_2O_3 overlayer, the surface niobium oxide overlayer is stable to calcination at elevated temperatures. The high-temperature stability of the surface niobium oxide overlayer on alumina is due to the strong interaction between the surface niobium oxide species and the alumina support as well as the high surface area of the Nb_2O_5/Al_2O_3 system. Crystalline $AlNbO_4$ and Nb_2O_5 phases are formed, however, at higher calcination temperatures and niobia concentrations, where the conditions are

Table 2
Influence of calcination temperature on surface area of supported niobium oxide on TiO_2 and Al_2O_3.

Sample	Calcination temperature[a]			
	500°C	700°C	850°C	950°C
TiO_2	56 m^2/g	31 m^2/g	12 m^2/g	–
5% Nb_2O_5/TiO_2	55 m^2/g	46 m^2/g	21 m^2/g	–
Al_2O_3	180 m^2/g	–	–	94 m^2/g
5% Nb_2O_5/Al_2O_3	178 m^2/g	–	–	99 m^2/g

[a] TiO_2 samples calcined for 2 h; Al_2O_3 sample calcined for 16 h.

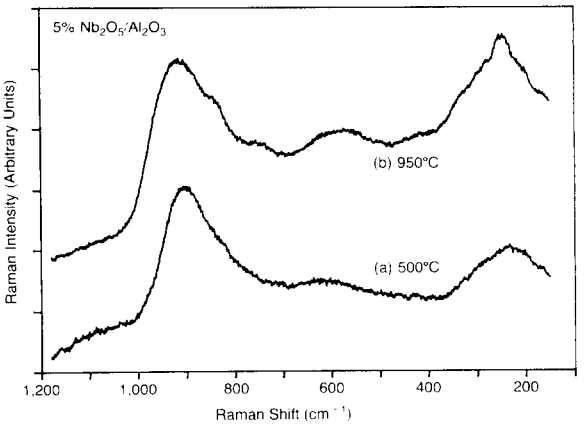

Fig. 9. Raman spectra for 5% Nb_2O_5/TiO_2 as a function of calcination temperature: (a) 500°C and (b) 850°C.

such that the surface niobium oxide concentration exceeds monolayer coverage and a portion of the supported niobium oxide phase is not directly interacting with the alumina surface. Thus, solid state transformations are retarded in the presence of surface niobium oxide overlayers on Al_2O_3.

The Raman spectra of the 5% Nb_2O_5/TiO_2 sample calcined at 500 and 850°C (see fig. 9) reveal that the surface niobium oxide overlayer is partially transformed to crystalline H–Nb_2O_5 (characteristic Raman band at 1000 cm^{-1}) by the high-temperature treatment. The weak Raman band at ≈890–940 cm^{-1} originates from the surface niobate overlayer also present in the 5% Nb_2O_5/TiO_2 (850°C) sample. The lower surface area of the 5% Nb_2O_5/TiO_2 (850°C) sample relative to 5% Nb_2O_5/Al_2O_3 (950°C) results in a surface coverage of the supported niobium oxide phase on TiO_2 beyond monolayer coverage, and transformed a portion of the surface niobate species to crystalline Nb_2O_5. At higher calcination temperatures the crystalline Nb_2O_5 reacts with the titania support to form several different Nb–Ti–O phases [17]. In contrast to the V_2O_5/TiO_2 system, the surface niobium oxide overlayer strongly interacts with the titania surface and is stable to high calcination temperatures. Furthermore, solid state transformations are retarded in the presence of surface niobium oxide overlayers on TiO_2 (i.e., transformation of TiO_2 (anatase) to TiO_2 (rutile), formation of crystalline Nb_2O_5 or Nb–Ti–O phases, and loss in surface area of TiO_2 support). The structural transformation in the Nb_2O_5/Al_2O_3 and Nb_2O_5/TiO_2 systems are schematically depicted in fig. 10.

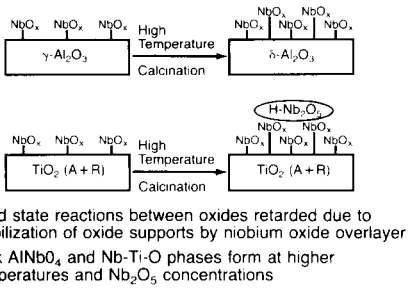

Fig. 10. Model of the interaction of niobium oxide with oxide supports.

3.3. Supported vanadium oxide and niobium oxide

The preceding studies demonstrate that the surface vanadium oxide overlayers and surface niobium oxide overlayers behave very differently at elevated temperatures. The surface vanadium oxide overlayers were found to be unstable to high calcination temperatures and to readily undergo solid state transformations. In contrast, the surface niobium oxide overlayers were found to be significantly more stable to high calcination temperatures and to retard solid state transformations. To determine if the stabilizing effect of the surface niobate overlayers could be incorporated into the unstable surface vanadate overlayers, several supported V_2O_5–Nb_2O_5 mixed samples were prepared and investigated. The V_2O_5–Nb_2O_5/TiO_2 system was chosen because of the extreme instability of the V_2O_5/TiO_2 system at intermediate calcination temperatures (450–600°C). Samples containing 8% V_2O_5 were prepared by impregnating a TiO_2 support containing 0–8% Nb_2O_5/TiO_2 and calcined at 575°C for 2 h.

The Raman spectra of the $V_2O_5/Nb_2O_5/TiO_2$ (575°C) samples are shown in fig. 11. The stronger Raman bands of the vanadium oxide component overshadow the weak Raman bands of the surface niobium oxide overlayer, and therefore the Raman bands of the supported vanadium oxide component are observed but not those due to the supported niobium oxide phase. In the absence of surface niobium oxide, the supported vanadium oxide phase exhibits a strong and sharp Raman band at 1000 cm^{-1} characteristic of crystalline V_2O_5, because

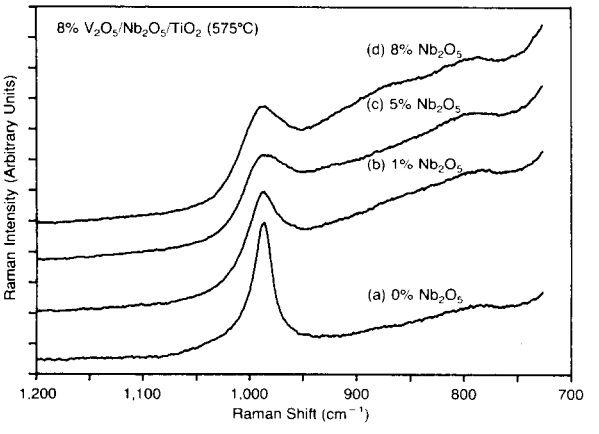

Fig. 11. Raman spectra for 8% $V_2O_5/Nb_2O_5/TiO_2$ (575°C) as a function of niobia coverage: (a) 0% Nb_2O_5, (b) 1% Nb_2O_5, (c) 5% Nb_2O_5, and (d) 8% Nb_2O_5.

Table 3
Surface niobium oxide phase thermally stabilizes the V_2O_5/TiO_2 system.

Sample	BET surface areas [a]
8% V_2O_5/TiO_2	21 m^2/g
8% V_2O_5/TiO_2 + 1% Nb_2O_5	43 m^2/g
8% V_2O_5/TiO_2 + 5% Nb_2O_5	43 m^2/g
8% V_2O_5/TiO_2 + 8% Nb_2O_5	46 m^2/g

[a] All samples calcined at 575°C for 2 h.

monolayer coverage is exceeded. In the presence of surface niobium oxide, the supported vanadium oxide phase exhibits a weak and broad Raman band characteristic of a surface vanadium oxide overlayer (see fig. 2). The corresponding surface areas of these $V_2O_5/Nb_2O_5/TiO_2$ samples are presented in table 3, and further reveal the stabilizing influence of the surface niobium oxide overlayer on the V_2O_5/TiO_2 systems. Thus, the presence of surface niobium oxide overlayers on TiO_2 retards the loss in surface area of V_2O_5/TiO_2 systems and the higher surface area, in turn, maintains the supported V_2O_5 phase as a surface vanadate overlayer. This property of surface niobium oxide overlayers is utilized in $V_2O_5/Nb_2O_5/TiO_2$ catalysts for NO_x emissions control from stationary sources [18].

4. Conclusions

The interaction of vanadium oxide and niobium oxide with Al_2O_3 and TiO_2 supports was examined with Raman spectroscopy. The Raman spectra of the supported metal oxides reveal that the strong interaction of the metal oxides with the Al_2O_3 and TiO_2 supports results in the formation of two-dimensional surface metal oxide overlayers. The overlayers possess at least two distinctly different surface metal oxide species, and their relative concentrations vary with surface coverage. The surface vanadium oxide overlayers are unstable at high calcination temperatures and accelerate the loss in surface area of the Al_2O_3 and TiO_2 supports. The surface vanadium oxide overlayer transformed to crystalline V_2O_5 on Al_2O_3 and to $V_xTi_{1-x}O_2$ (rutile) solid solution on TiO_2 at elevated temperatures. The surface niobium oxide overlayers are stable to high calcination temperatures and retard the loss in surface area of the Al_2O_3 and TiO_2 supports and solid state transformations. The surface niobium oxide is also found to stabilize the unstable surface vanadium oxide overlayer in mixed $V_2O_5/Nb_2O_5/TiO_2$.

Acknowledgement

Financial support by Niobium Products Company and the Pennsylvania Ben Franklin Technology Center is gratefully acknowledged.

References

[1] M.L. Deviney and J.L. Gland, eds., Catalyst characterization science, ACS Symposium Series 288 (American Chemical Society, Washington, 1985).
[2] I.E. Wachs, F.D. Hardcastle and S.S. Chan, Spectroscopy 1, No. 8 (1986) 30.
[3] I.E. Wachs and F.D. Hardcastle, Proc. 9th Intern. Congr. Catal. 3 (1988) 1449.
[4] W.P. Griffith and T.D. Wickins, J. Chem. Soc. A (1966) 1087.
[5] F. Roozeboom, J. Medema and P.G. Gellings, Z. Physik. Chem. (Frankfurt am Main) 111 (1978) 215.
[6] F. Roozeboom, M.C. Mittlemeijer-Hazeleger, J.A. Moulijn, J. Medema, V.H.J. de Beer and P.G. Gellings, J. Phys. Chem. 84 (1980) 2783.
[7] S.S. Chan, I.E. Wachs, L.L. Murrell, L. Wang and W.K. Hal, J. Phys. Chem. 88 (1984) 5831.
[8] I.E. Wachs, R.Y. Saleh, S.S. Chan and C.C. Chersich, Appl. Catal. 15 (1985) 339.
[9] R.Y. Saleh, I.E. Wachs, S.S. Chan and C.C. Chersich, J. Catal. 98 (1986) 102.
[10] H. Eckert and I.E. Wachs, Microstructure and properties of catalysts, Mater. Res. Soc. Symp. Proc. 111 (1988) 459.
[11] R. Grabowski, B. Grzybowska, J. Haber and J. Saloczynski, React. Kinet. Catal. Letters 2 (1975) 81.
[12] G.C. Bond, J. Sarkany and G.D. Parfitt, J. Catal. 57 (1979) 476.
[13] A. Vejux and P. Courtine, J. Solid State Chem. 23 (1978) 93.
[14] R. Kozlowski, R.F. Pettifer and J.M. Thomas, J. Phys. Chem. 87 (1983) 5176.
[15] A.A. McConnell, J.S. Anderson and C.N.R. Rao, Spectrochim. Acta 32A (1976) 1067.
[16] F.D. Hardcastle, I.E. Wachs, D.A. Jefferson, Z. Wuzong and J.M. Thomas, Colloid and Surface Chemistry Division, ACS Meeting, New Orleans, LA (Aug. 29–Sept. 5, 1987), paper no. 122.
[17] A.F. Wells, Structural inorganic chemistry (Oxford Univ. Press, London, 1984).
[18] H. Yoshida, S. Morikawa, K. Takahashi and M. Kurita, Japanese Patent No. 57-48342 (1982).